Journal of Chromatography A, 658 (1994) 445–457
Elsevier Science B.V., Amsterdam

CHROM. 25 617

Influence of lateral interactions on preparative protein chromatography

I. Isotherm behavior

Yong-Long Li and Neville G. Pinto*

Department of Chemical Engineering, University of Cincinnati, Cincinnati, OH 45221-0171 (USA)

ABSTRACT

A thermodynamically consistent adsorption equilibrium model based on the stoichiometric displacement principle has been developed for non-linear protein ion exchange. The adsorbed phase is modeled as a surface solution in equilibrium with an ideal bulk liquid, and non-idealities on the surface are calculated from surface activity coefficients. The model has been used to systematically investigate the influence of lateral interactions on equilibrium isotherms. Using experimental data for the ion exchange of bovine serum albumin, it has been shown that lateral interactions are a function of the adsorbed protein concentration, and this dependence strongly influences adsorption behavior. Lateral interactions on the surface have been found to be influenced by both energy of interactions between molecules and molecular shape, with the former being dominant. The relationships between lateral interactions, effective protein charge, and modulator concentration have also been investigated. Increases in adsorbate charge may result in an increase or decrease in adsorption capacity, depending on the relative concentration of the modulator, while increases in modulator concentration decrease capacity. For a complete characterization of salt effects, it is necessary to determine the dependence of isosteric heat of adsorption on salt concentration.

INTRODUCTION

In the past three decades, HPLC has played a prominent role in biotechnology, as an analytical technique, from the beginning, and, more recently, as an isolation and purification method [1]. Recognition of the potential of HPLC as a useful separation method at the process scale has generated a great deal of interest in non-linear (overload) chromatography, both in the elution [2–5] and displacement [6–11] modes of column development.

For modeling non-linear chromatographic separations of biomolecules, the Langmuir isotherm is frequently invoked. However, it has been observed that this isotherm often provides an unsatisfactory description of equilibrium adsorption behavior [12,13], and, furthermore, violates the Gibbs–Duhem law of thermodynamics [14,15]. Consequently, significant efforts are being made to develop thermodynamically consistent models for the adsorption of biomolecules on common adsorbents.

For the separation of biomolecules by ion-exchange chromatography, the stoichiometric displacement model (SDM) is of particular interest. This model is based on the assumption that ion exchange is the only mechanism for adsorption, and the ion-exchange process can be modeled as a stoichiometric "reaction" described by the mass-action principle. The model was originally proposed by Regnier and co-workers to correlate protein retention in linear ion-exchange chromatography [16,17]. More recently, SDM has been applied to overload protein

* Corresponding author.

0021-9673/94/$07.00
SSDI 0021-9673(93)E1057-7

chromatography. Regnier and Mazsaroff [18] used SDM equations to establish the implications of three-dimensional structure of macromolecules, non-ideal behavior in the liquid phase, and displacement effects between competing adsorbates during non-linear operation. Velayudhan and Horváth [19] in a theoretical analysis of SDM applied to multicomponent systems showed the effects of salt concentration and competitive binding on retention in the non-linear region. More recent applications of SDM to protein ion exchange have taken into consideration steric effects due the bulky nature of adsorbing protein molecules. This has been done by incorporating either an accessibility coefficient [20] or steric factor [21], and it has been shown that effects of size and shape can be effectively accounted for with SDM. The use of SDM in modeling chromatographic columns is very recent. Cysewski *et al.* [22] have simulated single protein isocratic and gradient elution with SDM to study the influence of protein charge and salt concentration on column performance. Bellot and Condoret [23] have extended this to binary mixtures of proteins. Finally, Brooks and Cramer [21] have applied SDM, with steric considerations included, to displacement separations.

In this paper we present a model for the multicomponent adsorption of large biomolecules by ion exchange. In common with the earlier contributions, this model is based on SDM. However, it incorporates lateral interactions on the surface, an effect previously neglected, and this effect is introduced in a thermodynamically rigorous manner. The model has been applied to the adsorption of bovine serum albumin (BSA) on an anion-exchange support. Relevant parameters have been experimentally measured for this system, and these are used as a basis for model predictions of adsorption isotherms.

THEORY

Model development

In this model we will consider the ion exchange of $n-1$ macromolecules, N_1, $N_2, \ldots, N_{n-1}$, in the presence of a small counter-ion (salt) N_n, called the modulator. As per SDM, the mechanism of adsorption is stoichiometric ion exchange with complete co-ion exclusion. For simplicity, the ion exchanger is assumed to have a constant ion-exchange capacity (*i.e.*, does not change with solution conditions), and the modulator is assumed to be univalent. With these considerations, the equilibrium distribution for the system is described by:

$$z_1 N_n^s + N_1 \rightleftharpoons z_1 N_n + N_1^s$$
$$z_2 N_n^s + N_2 \rightleftharpoons z_2 N_n + N_2^s$$
$$\vdots \qquad\qquad \vdots$$
$$z_{n-1} N_n^s + N_{n-1} \rightleftharpoons z_{n-1} N_n + N_{n-1}^s$$

For each of these ion-exchange "reactions", the equilibrium constants are related to the species activities by:

$$K_i = \frac{(a_n)^{z_i} a_i^s}{(a_n^s)^{z_i} a_i} \quad i = 1, \ldots, n-1 \tag{1}$$

In the adsorbed phase,

$$a_i^s = \gamma_i^s n_i^s \phi \quad i = 1, \ldots, n \tag{2}$$

where ϕ is the phase ratio. In the mobile phase,

$$a_i = \gamma_i c_i \quad i = 1, \ldots, n \tag{3}$$

In a rigorous application of this model it is necessary to include activity coefficients in the surface phase and bulk phase in the calculation of the equilibrium constant K_i. However, as a first approximation, we assume activity coefficients in the liquid are unity; *i.e.*, the liquid solution is ideal. Though this assumption is not in general justified, since in the overload mode concentrations in the liquid will be high, it serves as a first approximation on the basis of the relative magnitudes surface and fluid activity coefficients. In a typical situation, the surface concentration will be higher than the fluid concentration by a factor of about 10. Thus, surface activity coefficients can be expected to dominate in the calculation of K_i. With the ideal liquid assumption, eqn. 3 can be written as:

$$a_i \approx c_i \quad i = 1, \ldots, n \tag{4}$$

Substituting eqns. 2 and 4 in eqn. 1,

$$K_i = \frac{(c_n)^{z_i}\gamma_i^s n_i^s \phi}{(\gamma_n^s n_n^s \phi)^{z_i} c_i} \quad i = 1, \ldots, n-1 \tag{5}$$

By definition,

$$\sum_i^n n_i^s = n^s \tag{6}$$

where n^s is the total ion-exchange capacity of the adsorbent. Eqns. 5 and 6, in conjunction with an appropriate equation for the activity coefficients in the surface phase, constitute the equilibrium model for the multicomponent ion-exchange system under consideration.

It is possible to derive the multicomponent Langmuir isotherm from eqns. 5 and 6. Assuming that all the adsorbates (proteins and modulator) have the same effective charge ($z_i = z_j$), it can be shown that these equations reduce to:

$$n_i^s = \frac{n^s K_i c_i}{\frac{\gamma_i^s}{\gamma_n^s} c_n + \gamma_i^s \sum_{j=1}^{n-1} \frac{K_j c_j}{\gamma_j^s}} \quad i = 1, \ldots, n-1 \tag{7}$$

If it is further assumed that the modulator concentration is constant, we can define a coefficient:

$$b_i = \frac{K_i}{c_n} \tag{8}$$

Substituting eqn. 8 in eqn. 7:

$$n_i^s = \frac{n^s b_i c_i}{\frac{\gamma_i^s}{\gamma_n^s} + \gamma_i^s \sum_{j=1}^{n-1} \frac{b_j c_j}{\gamma_j^s}} \quad i = 1, \ldots, n-1 \tag{9}$$

It is now necessary to assume that the surface solution is ideal ($\gamma_i^s = 1$). Also, defining

$$g_i = b_i n^s, \quad i = 1, \ldots, n-1 \tag{10}$$

eqn. 9 simplifies to:

$$n_i^s = \frac{g_i c_i}{1 + \sum_{j=1}^{n-1} b_j c_j} \quad i = 1, \ldots, n-1 \tag{11}$$

This is the multicomponent Langmuir equation. The derivation of this equation demonstrates its limitation for non-linear ion-exchange chromatography. First, eqn. 11 requires that all adsorbates have the same effective charge. This is clearly inappropriate for protein ion exchange [6,16,20]. Secondly, the Langmuir coefficients are a function of the modulator concentration (eqns. 8 and 10). For chromatographic separations, this is a practical problem, since modulator gradients are generally present in the column. Even if the concentration dependence of the coefficients as specified by eqn. 8 is included, Velayudhan and Horváth [19] have shown that the Langmuir isotherm does not adequately characterize the influence of salt on protein binding. Thus, the assumption of an ideal surface phase, which removes the influence of the concentration dependence of the surface activity coefficients, is not appropriate. The ideal surface phase assumption also implies that all adsorbates are of about the same size and shape and have very similar intermolecular forces. The consideration of the characteristics of just the modulator–protein pair makes this assumption unreasonable.

Surface activity coefficients

A key requirement in the application of the model to the prediction or characterization of multicomponent ion-exchange equilibria is the availability of an appropriate method for the calculation of surface activity coefficients. This mandates a suitable model for the adsorbed phase. For protein ion-exchange chromatography, the adsorbed phase is made up of molecules of widely differing shapes and sizes. Also, lateral interactions between adsorbed molecules will be significant, since concentrations in the adsorbed phase are high. Furthermore, since protein molecules have ionic, polar, and non-polar regions, both short- and long-range interactions will, in general, be present.

Local composition models developed for multicomponent liquids solutions provide useful paradigms for the development of equivalent descriptions for adsorbed phases. Maurer and Prausnitz [24] have developed a local composition model for liquid mixtures made up of molecules of different sizes and shapes; their model is often referred to as the UNIQUAC

model. The UNIQUAC model is capable of estimating thermodynamic properties of liquid mixtures from essentially pure component data. This characteristic, and the fact that molecules of different sizes and shapes can be accommodated, makes UNIQUAC promising for adaptation for adsorbed protein mixtures; in this case, single-component adsorption isotherms are often the only data available. As developed by Maurer and Prausnitz [24], the UNIQUAC model is most appropriate for non-electrolyte mixtures since it accounts for only short-range interactions. More recently, however, Christensen and co-workers [25,26] have extended the model to electrolyte solutions by accounting for long-range forces with the Debye–Hückel theory. They have shown that with this modification the activity coefficients in concentrated, strong electrolyte solutions are well characterized. The ability to effectively account for long-range electrostatic interactions is another reason for exploring the potential applicability of the UNIQUAC model to adsorbed protein mixtures.

As has been discussed by Talu and Zwiebel [27], in adapting a liquid model to a surface phase, three requirements must be met. First, consistent with the usual selection of the standard state (pure component at the same temperature and spreading pressure as the mixture), the surface activity coefficient must satisfy the condition:

$$\lim_{x_i \to 1} \gamma_i^s = 1 \quad i = 1, \ldots, n \tag{12}$$

Also, as the spreading pressure approaches zero, the adsorbed solution approaches ideal behavior, and

$$\lim_{\pi \to 0} \gamma_i^s = 1 \quad i = 1, \ldots, n \tag{13}$$

This requires that surface activity coefficient equations be spreading pressure dependent. Finally, the activity coefficient equations must obey the Gibbs–Duhem relation. With these restrictions, Talu and Zwiebel [27] have adapted the UNIQUAC model to multicomponent adsorbed phases, and derived the following equation for surface activity coefficients:

$$\ln \gamma_i^s = -S_i \ln\left(\sum_{j=1}^{n} \omega_j \alpha_{ij}\right) + S_i - S_i \sum_{j=1}^{n} \frac{\omega_j \alpha_{ij}}{\sum_{k=1}^{n} \omega_k \alpha_{kj}} \quad i = 1, \ldots, n \tag{14}$$

where S_i is the adsorbate shape factor, and ω_j is the surface fraction defined as:

$$\omega_j = \frac{S_j x_j^s}{\sum_{k=1}^{n} S_k x_x^s} \tag{15}$$

α_{ij} is the Boltzmann weighting factor for local compositions. It is calculated using Wilson's method [28] for incorporating differences in intermolecular forces between components of the adsorbed phase. α_{ij} is related to the average lateral interaction energy between segments of nearest neighbor molecules (e_{ij} or e_{jj}) by:

$$\alpha_{ij} = \exp\left[-\frac{\sigma}{2}(e_{ij} - e_{jj})/kT\right] \tag{16}$$

where σ is the coordination number for the adsorbed segments. It is the energy of interaction parameters e_{jj} and e_{ij} that are functions of the spreading pressure. Talu [29] has shown that at low temperatures e_{jj} can be calculated from pure component isosteric heat of adsorption data:

$$e_{jj} = \frac{q_{j\pi}^{st} - q_{j0}^{st}}{\frac{\sigma}{2} MS_j} \tag{17}$$

where $q_{j\pi}^{st}$ is the isosteric heat of adsorption of pure j at the same spreading pressure as the mixture, and q_{j0}^{st} is the isosteric heat of adsorption at zero spreading pressure. The cross-energy parameters are calculated from:

$$e_{ij} = (e_{ii} e_{jj})^{1/2}(1 - \beta_{ij}) \tag{18}$$

where β_{ij} is an empirical factor that accounts for differences in size and adsorptive properties of the molecules.

In applying the UNIQUAC model to electrolyte solutions, Christensen *et al.* [25] calcu-

lated the molar excess Gibbs energy for the mixture from:

$$g^E = g^E_{DH} + g^E_{comb,LC} + g^E_{res,LC} \quad (19)$$

where g^E_{DH} is the Debye–Hückel contribution due to long-range interactions, $g^E_{comb,LC}$ is the combinatorial contribution from the local composition model, and $g^E_{res,LC}$ is the contribution from short-range interactions as calculated from the local composition model. In deriving eqn. 14 for adsorbed phases, Talu and Zwiebel [27] have only considered the $g^E_{res,LC}$ term in eqn. 19. Thus, using their equation for the calculation of surface activity coefficients of adsorbed protein mixtures is equivalent to neglecting features such as lateral ionic interactions on the surface, and the accessibility of ion-exchange sites due to size and shape of the molecule. Eqn. 14 accounts for only short-range lateral interactions, as between non-polar and polar segments of the adsorbates, and the influence of molecular shape on these interactions.

Though the general applicability of eqn. 14 is limited, it proves a thermodynamically sound basis for investigating the significance of lateral interactions for protein ion exchange. Furthermore, since this equation is rigorously derived and is consistent with eqn. 19, it serves as a first stepping stone in the systematic development of a more generally applicable equation for surface activity coefficients. Thus, for a preliminary investigation of the importance of lateral interactions, eqn. 14 was used in this study.

EXPERIMENTAL

Materials and apparatus

BSA was obtained from Sigma (St. Louis, MO, USA). Matrex PAE-1000 (a weak anion exchanger, 10 μm diameter, 1000 Å average pore size) was purchased from Amicon (Danvers, MA, USA), and was slurry packed into 0.46 cm I.D. columns of different lengths at a maximum pressure of 4000 p.s.i. (1 p.s.i. = 6894.8 Pa) with a Haskel air-driven pump (Alltech, Deerfield, IL, USA). Sodium chloride, silver nitrate, sodium azide and imidazole were all obtained from Aldrich (Milwaukee, WI, USA). Hydrochloric acid and methanol were bought from Fisher Scientific (Fair Lawn, NJ, USA). All reagents were used as received without further purification.

The chromatographic system for the frontal and elution experiments included a SP8800 gradient HPLC pump (Spectra-Physics, San Jose, CA, USA), a Model 2550 UV–Vis detector (Varian Instruments, Sunnyvale, CA, USA), and a HP 3396A integrator (Hewlett-Packard, Palo Alto, CA, USA). The column temperature was controlled with a Frigomix thermal bath (Melsungen, Germany).

Procedures

Effective protein charge. The effective charge (z_i) of BSA was measured by linear, isocratic elution on a 25 cm × 0.46 cm I.D. column. The column was first washed with 1.5 *M* salt solution for more than 30 min using a flow-rate of 1.0 ml/min. It was then equilibrated with the desired eluent, and 20 μl of BSA solution of concentration 0.5 mg/ml was injected. The BSA was isocratically eluted using a flow-rate of 1.0 ml/min. All the elutions were performed at pH 7 using 20 m*M* imidazole as the buffer, and the column temperature was maintained at 25°C. Sodium chloride was used as the salt, and the experiments were repeated at a number of salt concentrations in the range 0.15 to 0.45 *M*.

Isotherm measurements. BSA adsorption isotherms were measured at 6.1, 23.3 and 35.4°C using frontal chromatography on a 5.05 × 0.46 cm I.D. column. The resin mass and phase ratio of this column were obtained pycnometry. Prior to the frontal run, the column was washed with 1.5 *M* NaCl solution, and equilibrated with buffer at pH 7. A protein solution of known concentration in buffer was then injected into the column until breakthrough. The frontal experiments were performed at 0.15 ml/min. This was found to be a suitable flow-rate with respect to mass transfer characteristics.

Equilibrium constants. The equilibrium constants (K_i) for protein ion exchange were also determined by frontal chromatography, using procedures identical to those described above. In

this case, however, the protein concentration used was 0.5 mg/ml in buffer solution. At this low concentration, it was established that operation is in the linear region of the isotherm. The linear frontal experiments were performed at the same temperatures as the isotherm experiments.

RESULTS AND DISCUSSION

Isotherm coefficients

Predictions on the influence of lateral interactions will be more meaningful if the coefficients of eqns. 5, 6 and 15 are obtained experimentally. Also, an important consideration, one which will ultimately determine the practical utility of the model, is the ease with which the required coefficients can be independently measured. With the objective of demonstrating that simple methods for the measurement of model coefficients are available, and also to provide for realistic predictions of behavior, the ion exchange of BSA in the presence of Cl^- on PAE-1000, a macroporous anion-exchange support, was experimentally studied.

The model requires four coefficients: the effective charge of the protein, z_i, the equilibrium constant, K_i, the dependence of the isosteric heat of adsorption, $q_{i\pi}^{st}$, on the surface composition, and the shape factor S_i. Using isocratic elution experiments described earlier, the effective protein charge was obtained from the dependence of the capacity factor on salt concentration. Under linear conditions, for which it is reasonable to assume that the surface phase is ideal, it can be shown that [16]:

$$\log k_i' = I + z_i \log \frac{1}{c_n} \tag{20}$$

Shown in Fig. 1 is a plot of eqn. 20 for BSA at pH 7. From this plot an effective charge of 4.8 was calculated from linear regression of the data.

The equilibrium constants K_i were also obtained under linear conditions, but from frontal experiments. The values obtained are reported in Table I for three temperatures. In calculating these values from eqn. 5, 4.8 was used for the effective protein charge, and 360 (mequiv./g) for the total ion-exchange capacity; ion-exchange

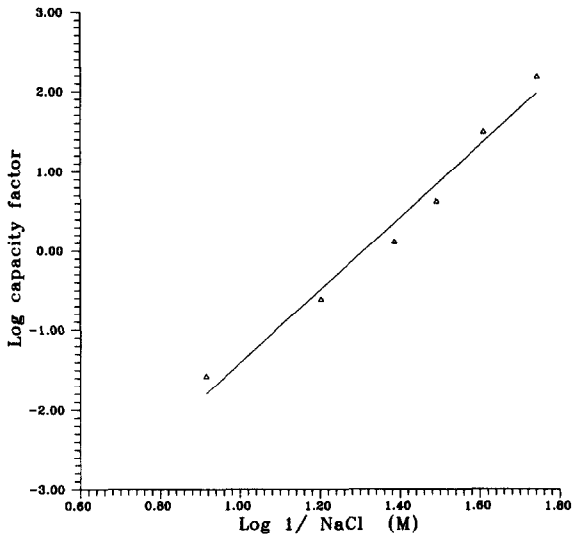

Fig. 1. Effective charge of BSA by linear chromatography. $z_i = 4.8$.

capacity data were provided by the manufacturer (Amicon).

The isosteric heat of adsorption for liquid adsorption has been obtained in the past [30] using the Clausius–Clapeyron type equation:

$$\frac{\partial(\ln c_i)}{\partial(1/T)} = \frac{q_{i\pi}^{st}}{R} \tag{21}$$

This is a convenient method for chromatography applications, since the only data necessary for the calculation are pure component isotherms, which can be conveniently measured from frontal experiments. However, the underlying assumption for eqn. 21 must be appreciated. In an analysis of the thermodynamics of adsorption of ionic systems, Parsons [31] and Betts and Pethica [32] have shown that eqn. 21 is only rigorously

TABLE I

EQUILIBRIUM CONSTANTS FOR BSA ION EXCHANGE AS A FUNCTION OF TEMPERATURE

Temperature (°C)	$K_{BSA} \cdot 10^6$
35.4	7.5
23.3	10.8
6.1	12.8

valid if the entropy of mixing is neglected and the adsorbed solution behaves like an ideal two-dimension gas. Clearly, these assumptions are not, in general, justified for protein ion exchange. However, because this study is a preliminary investigation to establish the importance of lateral interactions, eqn. 21 was used to determine $q_{i\pi}^{st}$. In the event that lateral interactions are established to be significant, it will be necessary in the future to make heat of immersion measurements to obtain more accurate estimates.

The adsorption capacities obtained with frontal chromatography for BSA on PAE-1000 at three temperatures are shown in Fig. 2. Also included in this figure are best fit curves for each temperature. On one of the fit curves, the model predicts an inflection point. However, this does not occur until a protein concentration of >50 mg/ml is reached. Since the best fit curves are based on experimental data up to a protein concentration of 40 mg/ml, this prediction is not considered reliable or significant.

The capacity measurements were made at a modulator (Cl^-) concentration of 15.5 m*M*. The maximum liquid concentration of protein used was 44 mg/ml, at which concentration the ion exchanger has a BSA capacity of between 120 and 160 mg/g, depending on temperature. This is in the range expected for this support, which has large pores of about 1000 Å size. Also as expected, the capacity decreases with increasing temperature, and this effect is more significant at higher coverages.

The isotherm data of Fig. 2 were used with eqn. 21 to calculate the isosteric heat of adsorption as a function of surface coverage. This was done by plotting ln c_i *versus* $(1/T)$ at constant n_i^s for a number of n_i^s values. the isosteric heats thus obtained are plotted as a function of coverage in Fig. 3. For the range studied, the $q_{i\pi}^{st}$ was found to be linearly dependent on the protein surface concentration. Also, the magnitude was between 0.7 and 1.1 kcal/mol (1 cal = 4.184 J), a reasonable range for physical adsorption. Linear regression of the experimental data was used to characterize the concentration dependence of $q_{i\pi}^{st}$, and extrapolation gave $q_{i\pi}^{st} = 1.95$ kcal/mol at zero protein concentration.

Rigorously, the $q_{i\pi}^{st}$ in eqn. 17 is the isosteric heat of adsorption for single component adsorption; *i.e.*, BSA has to be the only adsorbate on the surface. However, because of the electroneutrality requirement of ion exchange, BSA cannot adsorb on PAE-1000 in the absence of a

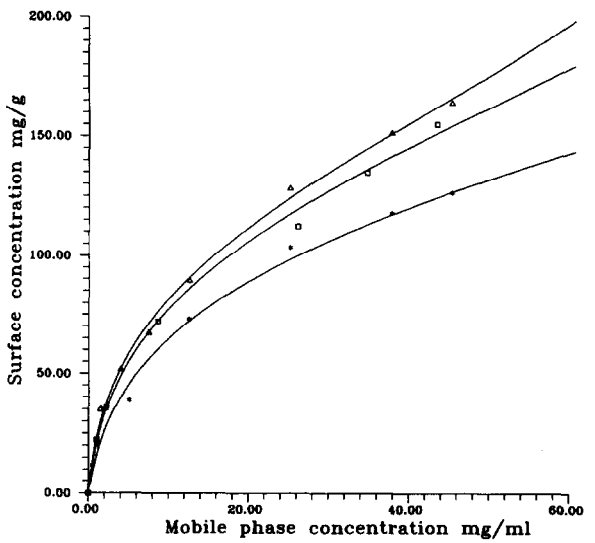

Fig. 2. Experimental adsorption isotherms for BSA on PAE-1000 at pH 7.0, 0.015 *M* Cl^-. (*) $T = 35.4$°C; $S_i = 4.2$; (□) $T = 23.3$°C; $S_i = 5.6$; (△) $T = 6.1$°C; $S_i = 6.4$.

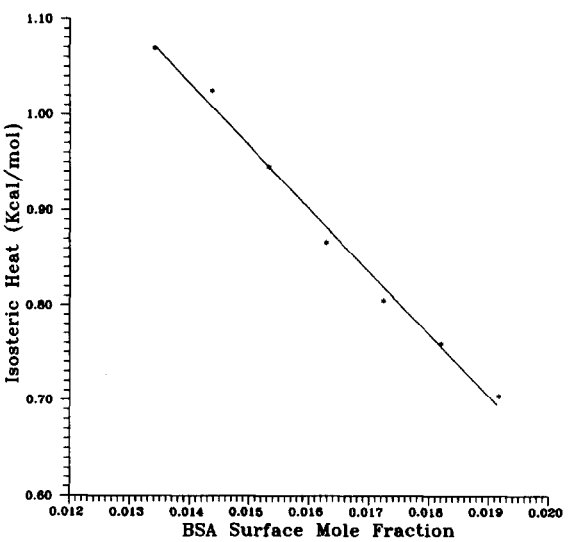

Fig. 3. Isosteric heat of adsorption for BSA as a function of coverage (same conditions as Fig. 2). $q_i^{st} = -65.8447x + 1.9544$.

counter ion. Under the experimental conditions used for the isotherm measurements, though no NaCl was added as a modulator, Cl^- originating from HCl in the buffer, added to adjust the pH, acts as the counter ion. This implies that the condition $\pi = 0$, in the strict sense of complete absence of adsorbates, is not realized for ion exchange. Thus, we define the zero spreading pressure state to be the ion exchanger saturated with Cl^- ions. With this definition, q_{i0}^{st} is the isosteric heat of adsorption at zero protein concentration, or $q_{i0}^{st} = 1.95$ kcal/mol.

An important inference can be made from the $q_{i\pi}^{st}$ data in Fig. 3. The magnitude of the energy indicates that lateral interactions are significant. In fact, they appear to be of about the same intensity as the primary ion-exchange interaction (*i.e.* with the fixed ionic sites). If it is assumed that lateral interactions between protein–Cl^- and Cl^-–Cl^- are negligible compared to protein-fixed ionic site and protein–protein interactions, the q_{i0}^{st} value provides a measure of the protein-fixed ionic site interaction. Thus, if lateral interactions between proteins were insignificant, the $q_{i\pi}^{st}$ would remain constant at q_{i0}^{st}. Though for the experimental range studied the $q_{i\pi}^{st}$ decreases linearly with increasing surface concentration, this trend cannot be expected to hold up to saturation. It is expected that as saturation is approached $q_{i\pi}^{st}$ will asymptotically approach a constant value; it should be noted that this condition could not be experimentally obtained because of solubility limitations for BSA in the liquid phase. In any case, if we conservatively assume that the asymptotic limit is the lowest value experimentally observed (≈0.7 kcal/mol), it is clear from the reduction of $q_{i\pi}^{st}$ (1.95 to 0.7 kcal/mol) that the strength of the lateral interactions is comparable to the primary ion-exchange interaction.

The final equilibrium coefficient necessary for the model is the shape factor S_i. This can be obtained by the fit of the single component isotherms with eqns. 5, 6 and 14, using the experimental values obtained for z_i (4.8), K_i (Table I), and $q_{i\pi}^{st}$ (Fig. 3). In this case, and for all subsequent analyses, the non-linear isotherm equations were solved with an equation solver using the Powell hybrid method [33]. The S_i fit values obtained are shown in Fig. 2. It is seen that the model characterizes the equilibrium behavior effectively at each temperature. Furthermore, S_i decreases with an increase in temperature.

As defined for eqn. 14, the shape factor is;

$$S_i = \frac{\text{free perimeter of molecule}}{\text{perimeter for standard segment}} \qquad (22)$$

Since the configurational and Debye–Hückel contributions are not included in eqn. 14, and the S_i values in Fig. 2 have been obtained from fits of the experimental isotherms, rigorous inferences about the significance of the values obtained cannot be made from eqn. 22. However, the magnitude and temperature dependence of S_i do provide some rough insight on the conformation of the protein on the surface. First, that data indicate that the conformation of adsorbed BSA changes with temperature, with a lower temperature resulting in more contact between the molecule and the adsorbed surface. Secondly, from the magnitudes of S_i, between 4 to 7 segments of BSA interact with the adsorbent. Also, the S_i value at 23.3°C, 5.6, is strikingly close to the z_i value of 4.8, which was obtained at 25°C. This makes it tempting to speculate that each segment interacting with the surface has, roughly, a unit negative charge, and, further, the variation of S_i with temperature suggests that z_i may be dependent on temperature. For this work, z_i has been assumed to be independent of temperature, but the results above have initiated a more detailed investigation, the results of which will be reported in a future communication.

Isotherm behavior

Using the model coefficients obtained above, the equilibrium model was used for a parametric study of adsorption isotherms. In order to illustrate the influence of lateral interactions on adsorption behavior, simulations were performed for various $q_{i\pi}^{st}$ values keeping all other coefficients constant at the values of BSA. The results obtained at 35.4°C are shown in Fig. 4. As a reference, the experimental data for BSA are shown, as is the model correlation with the experimental $q_{i\pi}^{st}$ data (Fig. 3).

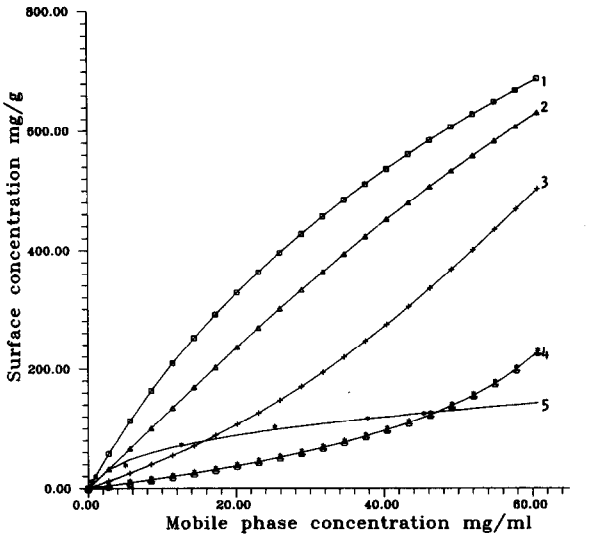

Fig. 4. Predicted effect of lateral interactions on BSA adsorption isotherm. (*) BSA isotherm, $T = 35.4$°C; $q_{i\pi}^{st} - q_{i0}^{st}$ = (1) 0.0; (2) −0.4; (3) −1.0; (4) −1.6 kcal/mol; (5) $q_{i\pi}^{st} - q_{i0}^{st}$ experimental.

Generally, lateral interactions are ignored in characterizations of isotherm data. This is equivalent to assuming that $q_{i\pi}^{st} - q_{i0}^{st} = 0$. With this constraint, the surface activity coefficients go to unity, and the model reduces to the original form of SDM [19]. It is clear from Fig. 4 that with $q_{i\pi}^{st} - q_{i0}^{st} = 0$ the model severely over-predicts the protein capacity. Correcting for this over-prediction by changing the z_i value is possible, but the significance of z_i is lost, and extensions to multicomponent mixtures are not possible. Also shown in Fig. 4 are three predictions at non-zero values of $q_{i\pi}^{st} - q_{i0}^{st}$. In each case, the $q_{i\pi}^{st} - q_{i0}^{st}$ is assumed to be independent of the surface coverage, in contrast to the experimental data for BSA. It is seen that as $q_{i\pi}^{st} - q_{i0}^{st}$ becomes more negative, that is, as repulsive lateral interactions get stronger, the protein capacity decreases. Also, the curve for $q_{i\pi}^{st} - q_{i0}^{st} = -1.0$ kcal/mol shows that the experimental data cannot be effectively characterized by an "average" value of $q_{i\pi}^{st} - q_{i0}^{st}$ within the experimental range; as will be shown later the model is not as sensitive to S_i as it is to $q_{i\pi}^{st}$, and it is not possible to fit the experimental data by adjusting the S_i within physically realistic values. Thus, it is essential to incorporate the composition dependence of $q_{i\pi}^{st}$.

Fig. 4 reveals one other important influence of lateral interactions on adsorption behavior. For $q_{i\pi}^{st} - q_{i0}^{st}$ values of −1.6 kcal/mol and −1.0 kcal/mol, the model predicts isotherms that are convex with respect to the x axis; *i.e.*, the isotherm has changed shape from Type I to Type III. The implication of this for overload elution is that it is now possible to explain fronting peaks (front boundary is diffuse and the rear is sharp) on the basis of lateral interactions on the surface; prior to this result, it was not possible to characterize such peaks with SDM. Clearly, lateral interactions can profoundly influence the behavior of proteins under overload conditions by fundamentally changing the shape of the isotherm.

All the simulations in Fig. 4 were done for negative or zero values of $q_{i\pi}^{st} - q_{i0}^{st}$, which correspond to repulsive lateral interactions or the absence of lateral interactions. If lateral interactions are attractive, it is to be expected that adsorption capacity will increase with increasing coverage. This is indeed what the model predicts, as is shown in Fig. 5.

According to the model, the magnitude of lateral interactions is dependent on the energies

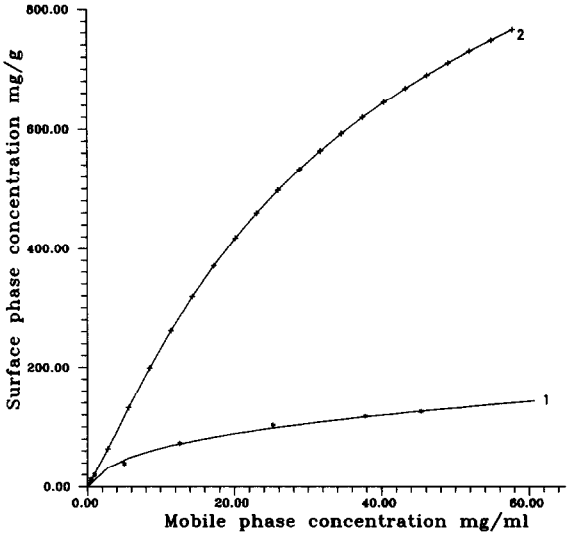

Fig. 5. Predicted effect of attractive lateral interactions on BSA adsorption isotherm. (*) BSA isotherm, $T = 35.4$°C; (1) $q_{i\pi}^{st} - q_{i0}^{st} = -65.13x$; (2) $q_{i\pi}^{st} - q_{i0}^{st} = 5.15x$.

of interaction (eqns. 14 and 17) and on the shape of the molecule (eqn. 14). Manipulations with $q_{i\pi}^{st} - q_{i0}^{st}$ in Figs. 4 and 5 illustrated only the influence of the energies of interaction. It is also of interest to establish the importance of shape factor. From Fig. 2 it is seen that S_i does have an influence on the adsorption isotherm, with larger values giving higher capacities. However, the isotherms are much less sensitive to S_i than they are to the energy of interaction. A fundamental change in the type of the isotherm can only be achieved with very large values of S_i. For example, in Fig. 6 it has been shown that with a S_i value of 60.25 the isotherm is no longer concave with respect to the x axis; in fact, an S-shaped isotherm is obtained. However, the value of S_i needed to generate this isotherm is not physically realistic, as evidenced by the very large protein capacities predicted. For physically realistic values of S_i, the capacity does change with S_i (Fig. 2), but the isotherm maintains the Type I shape. Thus, it can be concluded that the energy of interaction is of primary importance for lateral interactions, and the shape of the molecule, though important, is a secondary influence.

The equilibrium model was also used to study the influence of z_i on the adsorption isotherm. Shown in Fig. 7 are the predictions at 35.4°C.

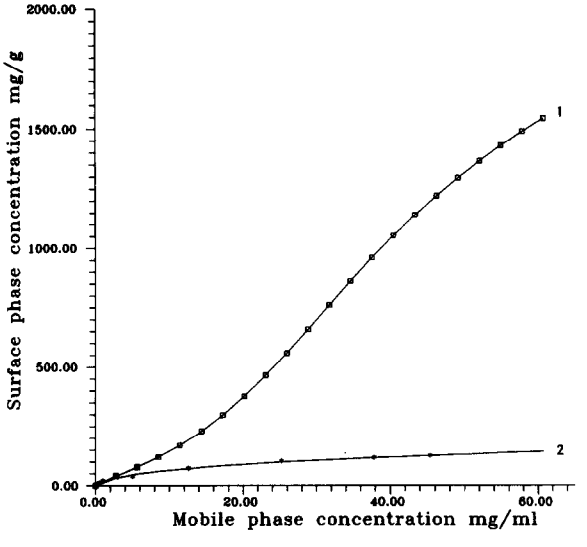

Fig. 6. Predicted effect of shape factor on BSA adsorption isotherm. (*) BSA, $T = 35.4$°C; shape factors: (1) 4.15, (2) 60.25.

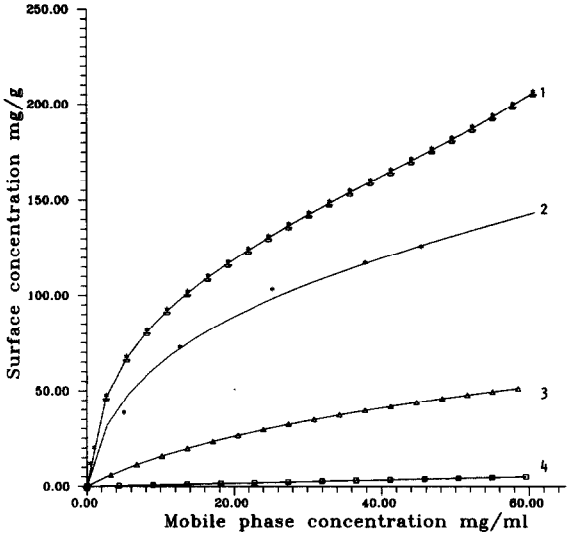

Fig. 7. Predicted influence of the effective charge on BSA adsorption isotherm. (*) BSA, $T = 35.4$°C; (1) $z_i = 5.0$; (2) $z_i = 4.8$; (3) $z_i = 4.0$; (4) $z_i = 3.0$.

The model predicts a strong dependence of capacity on z_i, with capacity decreasing rapidly with a decrease in protein charge. However, this behavior is very dependent on the modulator concentration relative to the total ion-exchange capacity of the support. In Fig. 7, calculated at experimental conditions of the BSA isotherm measurements, the modulator concentration is low (15.5 mM) relative to the ion-exchange capacity (360 mequiv./g). Shown in Fig. 8 is the dependence when the modulator concentration is high (210 mM) relative to the total capacity (200 mequiv./g). In this case, the protein with the lower z_i is more effective in displacing counter ions from the surface, and, thus, gives a higher capacity. The difference in behavior can be explained qualitatively as follows. At conditions under which the modulator to fixed-site ratio is relatively low, it is easy for the protein molecules to simultaneously displace the required number of modulator ions from the surface, because completion with the modulator ions is low due to their low concentration. Thus, for two proteins with the different z_i, the strong binding affinity of the protein with the higher z_i gives it a higher capacity. In contrast, when the modulator to fixed-site ratio is relatively high, the competition for sites is stiff, and proteins that have to

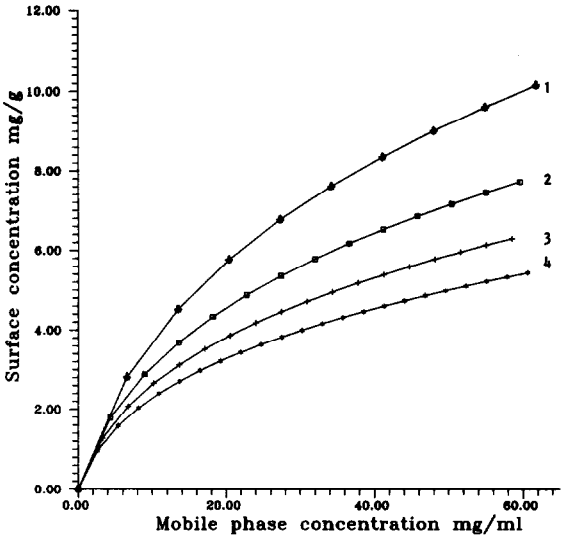

Fig. 8. Predicted influence of effective charge at low capacity to modulator concentration ratio. (1) $z_i = 2.0$; (2) $z_i = 3.0$; (3) $z_i = 4.0$; (4) $z_i = 5.0$.

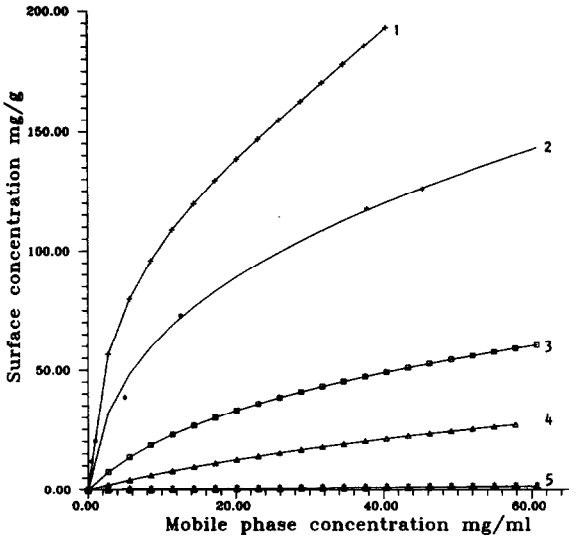

Fig. 9. Predicted effect of modulator concentration on BSA adsorption isotherm. (*) BSA, $T = 35.4$°C; modulator concentrations: (1) 12.5 mM; (2) 15.5 mM; (3) 23.3 mM; (4) 31.0 mM; (5) 62.0 mM.

displace a large number of modulator ions are less likely to adsorb.

For overload protein ion-exchange chromatography operated in the displacement mode, the salt/fixed-site ratio in Fig. 7 is typical. It is interesting to note that in this case the model predicts, with the operating line approach [6], that proteins with larger charge will displace those with a lower charge, all other factors being the same. This is consistent with experimental data reported in the literature for the displacement of proteins with polyelectrolytes [11].

The final characteristic studied with the equilibrium model is the influence of modulator concentration. The predictions are shown in Fig. 9. A very strong dependence on concentration of the modulator is predicted. In fact, the model predicts too strong a dependence. At a modulator concentration of 62 mM, the support is predicted to have essentially no capacity for the protein. This is inconsistent with the experimental results, which show significant retention for BSA at much higher concentrations (Fig. 1). The problem appears to be neglect of the influence of salt concentration on the isosteric heat of adsorption. The isotherm measurements (Fig. 2) were made at a single modulator concentration (15.5 mM), and, therefore, in all likelihood, the experimental $q_{i\pi}^{st} - q_{i0}^{st}$ function of Fig. 3 does not adequately incorporate the influence of the modulator concentration.

In order to illustrate how a dependence of $q_{i\pi}^{st} - q_{i0}^{st}$ on modulator concentration can affect the isotherm, simulations were performed with the linear function in Fig. 3, but for various values of the "slope" coefficient; changes in this coefficient with modulator concentration are one possible scenario for the effects of modulator. The simulation were performed for a modulator concentration of 23.3 mM, and the results are shown in Fig. 10; as a reference, the curve using the experimental $q_{i\pi}^{st} - q_{i0}^{st}$ function obtained at 15.5 mM is also shown ($-65.85x$). Clearly, the adsorption capacity is strongly affected, with the capacity increasing as the repulsive lateral interaction energy is decreased. This result, the results in Fig. 9, and the experimental capacity factor data (Fig. 1), suggest that increases in modulator concentration tend to reduce lateral interactions between adsorbed proteins. A general implication of this result is that if the model is to be used in situations that involve modulator gradients, a complete characterization of $q_{i\pi}^{st} - q_{i0}^{st}$ in the composition space of interest is necessary.

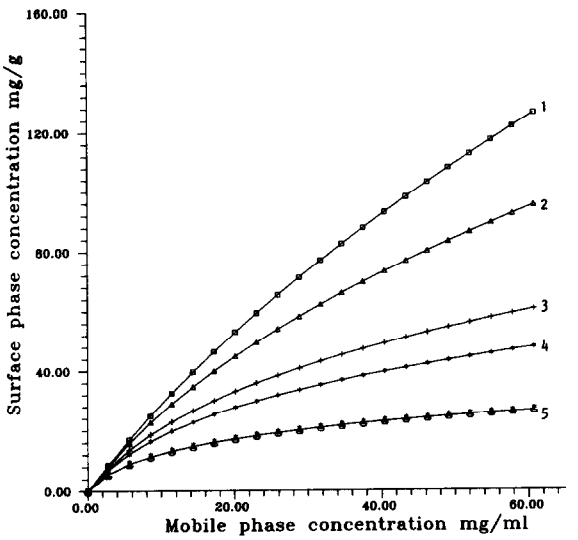

Fig. 10. Influence of lateral interactions on adsorption isotherm. Modulator concentration: 23.3 mM. $q_{i\pi}^{st} - q_{i0}^{st} = (1) -10.13x$; (2) $-25.13x$; (3) $-65.85x$; (4) $-100.0x$; (5) $-250.0x$.

CONCLUSIONS

An equilibrium model has been presented for the ion exchange of proteins. This model extends SDM by incorporating lateral interactions between adsorbed molecules. This is done using a local composition model for the surface. The model involves four equilibrium coefficients: the effective protein charge, the equilibrium constant, isosteric heat of adsorption, and a molecular shape factor. It has been shown that each of these coefficients can be measured solely from chromatographic experiments.

Using the ion exchange of BSA as a model, a parametric study revealed that lateral interactions can profoundly affect the equilibrium isotherm. The strength of the lateral interactions is influenced by the energy of interaction and the shape of the molecule. However, the adsorption equilibrium is much more sensitive to the interaction energy, and it is essential to establish its composition dependence in order to achieve an effective characterization.

The present effort represents only the first step in developing a thermodynamically consistent description of protein ion exchange for nonlinear chromatography. In its present form, configurational contributions and long range interactions are lumped together with short-range interactions. Though this approach is practically convenient, whether it works for chromatographic separations needs to be established. In particular, it has to be determined whether parameters obtained from single component data have validity for multicomponent separations. If found to be not generally valid, explicit terms for long-range interactions and configurational effects will have to be included in order to exploit the full potential of this approach.

SYMBOLS

a_i	activity
b_i	Langmuir coefficient
c_i	mobile phase concentration
e_{ij}	lateral interaction potential between segment of molecules i and j
g_i	Langmuir coefficient
g^E	excess Gibbs free energy
I	intercept
k	Boltzmann constant
K_i	equilibrium constant
M	Avogadro number
n	number of species
n^s	total ion-exchange capacity
n_i^s	concentration of species i on surface
N_i	adsorbate i
$q_{i\pi}^{st}$	isosteric heat of adsorption at spreading pressure π
q_{i0}^{st}	isosteric heat of adsorption at zero spreading pressure
R	universal gas constant
S_i	shape factor
T	absolute temperature
x_i	adsorbate mole fraction
z_i	effective charge
α_{ij}	Boltzmann weighting factors for local segment compositions
β_{ij}	empirical factor
ϕ	phase ratio
ω_j	surface fraction
γ	activity coefficient
π	spreading pressure
σ	coordination number

Subscripts

DH	Debye–Hückel contribution
comb, LC	combinatorial contribution from the local composition model
i, *j*, *k*	indices for components
n	modulator
res, LC	residual contribution from local composition model

Superscript

s	surface phase

REFERENCES

1 F.E. Regnier, *Chromatographia*, 24 (1987) 241.
2 Y.B. Yang, K. Harrison, D. Carr and G. Guiochon, *J. Chromatogr.*, 590 (1992) 35.
3 G.B. Cox and L.R. Snyder, *J. Chromatogr.*, 590 (1992) 17.
4 G. Cretier, M. El Khabchi and J.L. Rocca, *J. Chromatogr.*, 596 (1992) 15.
5 A. Felinger and G. Guiochon, *J. Chromatogr.*, 591 (1992) 31.
6 J. Frenz and Cs. Horváth, in Cs. Horvath (Editor), *High-Performance Liquid Chromatography —Advances and Perspectives*, Vol. 5, Academic Press, New York, 1985, p. 211.
7 G. Subramanian, M.W. Phillips and S.M. Cramer, *J. Chromatogr.*, 439 (1988) 341.
8 A.R. Torres and E.A. Peterson, *J. Chromatogr.*, 604 (1992) 39.
9 K. Kalghatgi, I. Ferregvári and Cs. Horváth, *J. Chromatogr.*, 604 (1992) 47.
10 S.-C.D. Jen and N.G. Pinto, *J. Chromatogr.*, 519 (1990) 87.
11 S.-C.D. Jen and N.G. Pinto, *J. Chromatogr. Sci.*, 29 (1991) 478.
12 P.K. de Bokx, P.C. Baarslag and H.P. Urbach, *J. Chromatogr.*, 594 (1992) 9.
13 P. Jandera and G. Guiochon, *J. Chromatogr.*, 605 (1992) 1.
14 C. Kemball, E.K. Rideal and E.A. Guggenheim, *Trans. Farad. Soc.*, 44 (1948) 948.
15 D.M. Ruthven, *Principles of Adsorption and Adsorption Processes*, Wiley, New York, 1984.
16 W. Kopaciewicz, M.A. Rounds, J. Fausnaugh and F.E. Regnier, *J. Chromatogr.*, 266 (1983) 3.
17 M.A. Rounds and F.E. Regnier, *J. Chromatogr.*, 283 (1984) 37.
18 F.E. Regnier and I. Mazsaroff, *Biotech. Prog.*, 3 (1987) 22.
19 A. Velayudhan and Cs. Horváth, *J. Chromatogr.*, 443 (1988) 13.
20 R.D. Whitley, R. Wachter, F. Liu and H.L. Wang, *J. Chromatogr.*, 465 (1989) 137.
21 C.A. Brooks and S.M. Cramer, *AIChE J.*, 38 (1992) 1969.
22 P. Cysewski, A. Jaulmes, R. Lemque, B. Sebille, C. Vidal-Madjar and G. Jilge, *J. Chromatogr.*, 548 (1991) 61.
23 J.C. Bellot and J.S. Condoret, *J. Chromatogr.*, 635 (1993) 1.
24 G. Maurer and J.M. Prausnitz, *Fluid Phase Equilibria*, 2 (1978) 9.
25 C. Christensen, B. Sander, A. Fredenslund and P. Rasmussen, *A Local Composition Model for Completely Dissociated Electrolyte Mixtures, SEP 8211*, Institute for Kemiteknik, Tekniske Hojskole, Lyngby, 1982.
26 C. Christensen, *Thermodynamics of Electrolyte and Development of a New Model for Electrolyte Mixtures, SEP 8203*, Institute for Kemiteknik, Tekniske, Hojskole, Lyngby, Denmark, 1982.
27 O. Talu and I. Zwiebel, *AIChE J.*, 32 (1986) 1263.
28 G.M. Wilson, *J. Am. Chem. Soc.*, 86 (1964) 127.
29 O. Talu, *Ph.D. dissertation*, Arizona State University, Tempe, AZ, 1984.
30 S. Jacobson, S. Golshan-Shirazi and G. Guiochon, *J. Chromatogr.*, 522 (1990) 23.
31 R. Parsons, *Can. J. Chem.*, 37 (1959) 308.
32 J.J. Betts and B.A. Pethica, *Trans. Faraday Soc.*, 56 (1960) 1515.
33 D. Kahaner, C. Moler and S. Nash, *Numerical Methods and Software*, Prentice Hall, Englewood Cliffs, NJ, 1989.